

ADAPTATION OF THE MAGNETIC PULSE METHOD FOR CONDUCTIVE MATERIALS TESTING

S.G. Magazinov*, S.I. Krivosheev, Yu.E. Adamyan, D.I. Alekseev, V.V. Titkov,

L.V. Chernenkaya

Peter the Great St.Petersburg Polytechnic University; Saint Petersburg, Russia

*e-mail: magazinov_sg@mail.ru

Abstract. The paper presents the results of experimental testing by magnetic-pulse method of Cu-ETP samples with crack type macro defect. Three-dimensional modeling of the magnetic field in the loading device -sample system was performed, on the basis of which the magnetic pressure was calculated and mechanical simulation was performed with Johnson-Cook plasticity model and fracture criteria. Comparison of the obtained results of residual deformation indicates the applicability of Johnson Cook plasticity model for OFHC copper for describing the behavior of Copper ETP in the deformation rate range up to 10^4 1/s.

Keywords: high speed deformation, magnetic-pulse loading, Johnson-Cook plasticity model

1. Introduction

Using of the magnetic-pulse method for creation controlled pressure pulses with microsecond duration for study of pulse strength of brittle nonconductive materials allowed to reveal a number of general consistent patterns of deformation process [1, 2, 3]. Applying of the thermodynamic approach for analysis of the results allowed to obtain the characteristic relation between extreme deformation loads and their duration, and specific for each material parameter - the time of energy accumulation [4]. Main feature of magnetic-pulse method of loading is the ability to form stress states, in which there are no loading modes with preliminary material compression, typical for spalling deformation tests. The realization of this feature is especially important in the testing of composite and laminate materials with an explicit spatial anisotropy of deformation characteristics.

The aim of the work is to substantiate and experimentally confirm the possibility of testing conductive samples in high-speed deformation modes and to identify possible limitations associated with the influence of the current induced in the sample on the deformation curves of the metal.

2. Pressure forming by the magnetic-pulse loading

The use of magnetic-pulse method, described in [4], for forming a load on a conducting sample can lead to a change in the ratios of the current pulse parameters flowing along the magnetic-pulse driver (hereinafter MPD) and the parameters of the pressure transferred to the sample.

The impact of conducting sample presence was studied with the use of numerical simulation in the environment Comsol Multiphysics. Process of generating a magnetic field in a MPD-sample system with geometric dimensions corresponding to dimensions of the sample used in the experiment. Simulation was performed for the MPD with length 15 mm. The main view of test sample with installed MPD is shown in Fig. 1.

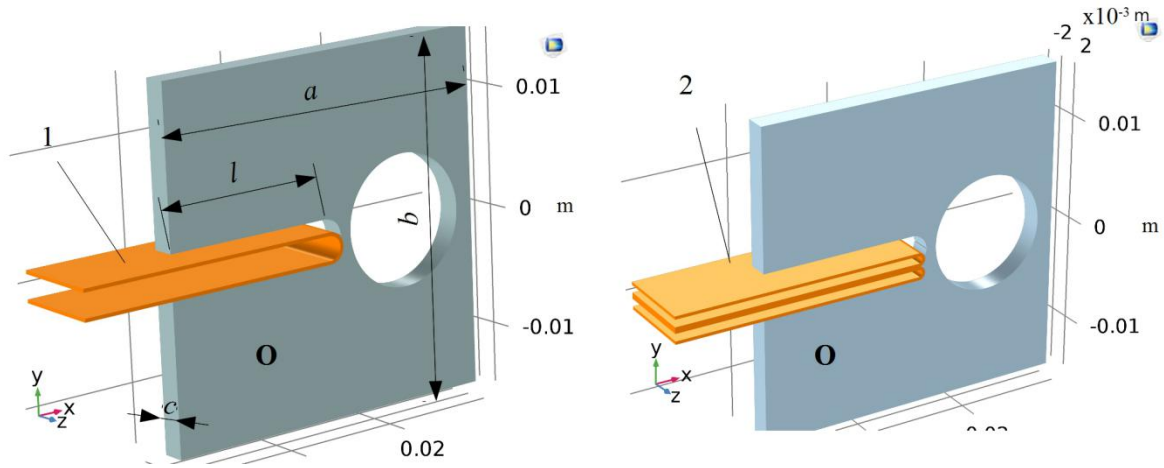


Fig. 1. Test sample (O) with installed magnetic-pulse driver (insulation is not shown)

The results of magnetic field simulation for simple and quasi-coaxial MPD with the width $c_{mpd}=7.8$ mm and samples with different conductivity are shown in Fig. 2.

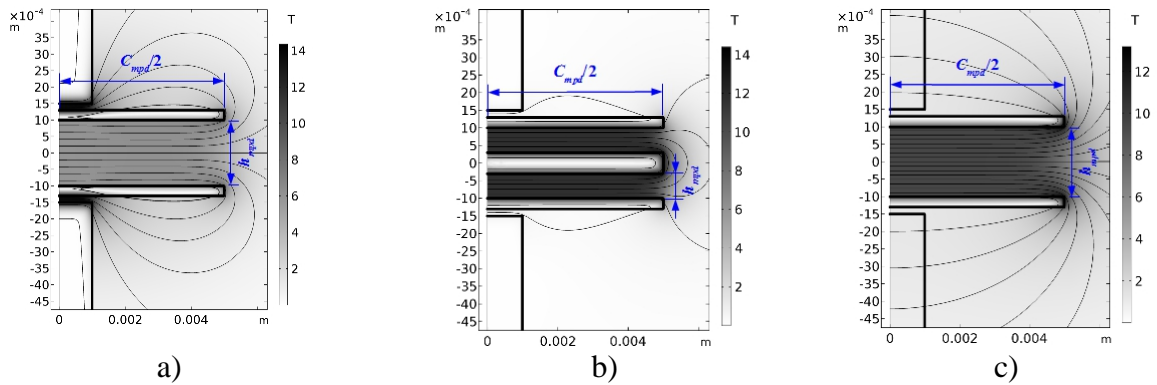


Fig. 2. Distribution of magnetic field induction at the moment of current maximum: a) simple MPD, conductive sample; b) quasi-coaxial MPD, conductive sample; c) simple MPD, conductive sample

Analysis of the results revealed some influence of the MPD width on the parameters of the pressure acting on the sample. This is due to the fact that in the system of flat busbars, under condition $c_{mpd} \gg h_{mpd}$, magnetic pressure P_m is related to the MPD current I with a simple relation:

$$P_m = \mu_0 \cdot (I/c_{mpd})^2 / 2, \quad (1)$$

where $\mu_0 = 4\pi \cdot 10^{-7}$ H/m, but this condition is not always satisfied during the experiment. Real relations between ratio of magnetic pressure acting on the groove and calculated with the use of (1), during the impulse current flowing through MPD

$$i(t) = I_m \sin\left(\frac{2\pi t}{T}\right) \quad (2)$$

with the period $T=8 \mu s$, close to the experimental one, and geometry parameters of MPD are shown in Fig. 3. Simulation was provided varying the width of MPD c_{mpd} and saving the value of current density $I_m/c_{mpd} = 10$ kA/mm, where I_m - amplitude value of current for test

sample with thickness $c=2$ mm, width and length $b=a=30$ mm, height of the groove $h=3$ mm, length of the groove $l=15$ mm (Fig. 1).

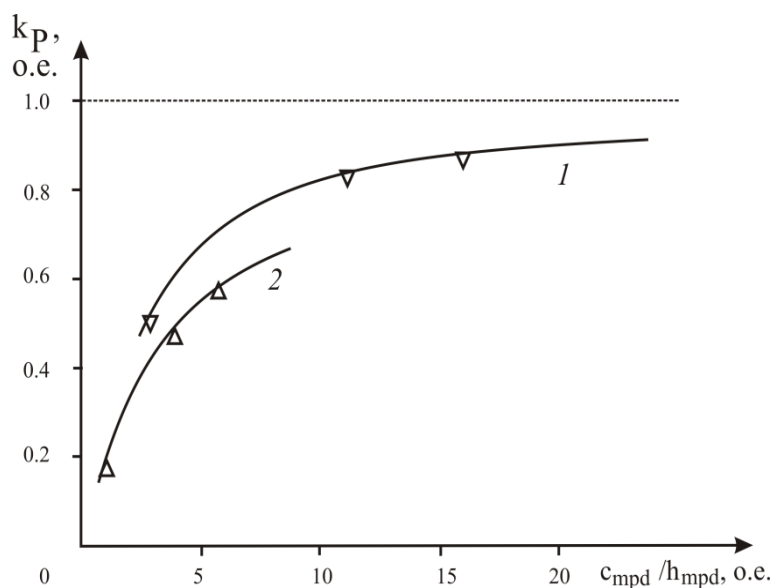


Fig. 3. Relations between ratio of magnetic pressure acting on the groove and calculated with the use of (1) and ratio of MPD busbars width and length between those busbars; 1 – simple MPD, 2 – quasi-coaxial MPD

The relations shown in Fig. 3 reveal that the increase of ratio c_{mpd}/h_{mpd} makes closer magnetic pressure to the pressure calculated with the use of (1). Since the calculation was performed for the experimental configuration of the sample, where groove height is constant, magnetic pressure formed by quasi-coaxial MPD exceeds the pressure formed by simple MPD with the same current in the branch of MPD.

3. Process of sample deformation under pulse loading

The simulation of elastic–plastic deformation of a copper busbar with macro defect of type of crack in the three-dimension setting was carried out using the ANSYS Autodyn environment [5]. Johnson-Cook (JC) plasticity model for OFHC copper [6] was selected as a calculation model of deformation.

JC plasticity model describes deformation process up to fracture, and the validity of use of JC plasticity model is confirmed by the good correspondence between calculated and experimental deformation curves for different plastically deformable materials at strain rates up to ~ 2000 1/s. The reliability of mentioned model for various metals is supported by its implementation in different programming environments, e.g. [5]. For instance, the applicability of JC model for description of the high-speed deformation process for steel 09G2S at strain rates up to 1500 1/s is shown in [7].

According to JC model the elastic limit of material varies depending on plastic strain, strain rate v_p , which must be equal or more then 1 s^{-1} , and temperature is described by the next expression

$$\sigma = [A + B\varepsilon_p^n] \cdot [1 + C \ln \dot{\varepsilon}_p^*] \cdot [1 - T^{*m}], \quad (3)$$

where ε_p – is an effective plastic strain, $\dot{\varepsilon}_p^* = \dot{\varepsilon}_p/\dot{\varepsilon}_p^0$ is a standardized effective plastic strain rate ($\dot{\varepsilon}_p^0 = 1 \text{ s}^{-1}$), T^* is homologous temperature

$$T^* = (T - T_{room}) / (T_{melt} - T_{room}), \quad (4)$$

$A = 90$ MPa, $B = 292$ MPa, $n = 0.31$, $C = 0.025$, $m = 1.09$, $T_{melt} = 1082.9^\circ\text{C}$ are model parameters.

JC fracture model similar to plasticity model is applied as the failure criterion:

$$D = \sum \frac{\Delta \varepsilon}{\varepsilon^f}, \quad (5)$$

$$\varepsilon^f = \left[D_1 + D_2 e^{D_3 \sigma^*} \right] \cdot \left[1 + D_4 \ln \dot{\varepsilon}_p^* \right] \cdot \left[1 + D_5 T^* \right], \quad (6)$$

where ε^f is an effective fracture strain, $D_1 = 0.54$, $D_2 = 4.89$, $D_3 = -3.03$, $D_4 = 0.014$, $D_5 = 1.12$ – deformation model parameters. When the parameter D reaches the value 1, the material is destroyed.

As it is presented in [8], the character of the stress state is defined by the characteristic size of the sample b and the loading wavelength $\lambda = c_1 T$, where the condition $\lambda \ll b$ allows to realize a shock-wave mode of loading, otherwise quasi-static mode. Maximum von Mises stress forms in the zone near the top of the groove at uniform distribution of pulse pressure.

Deviation of deformation curve from linear as a result of plastic flow leads to sufficient reduce of acceptable stress, as it is shown in figure 4a in the case of shock-wave loading mode (curves 1, 2, 3). Herewith it is not possible to ensure high strain rate $\dot{\varepsilon}_p$ (Fig. 4). Transition to the quasi-static loading mode allows to expand the range of reachable stress and ensure greater deformations of material in the top of the groove, up to the fracture (Fig. 4, curve 4).

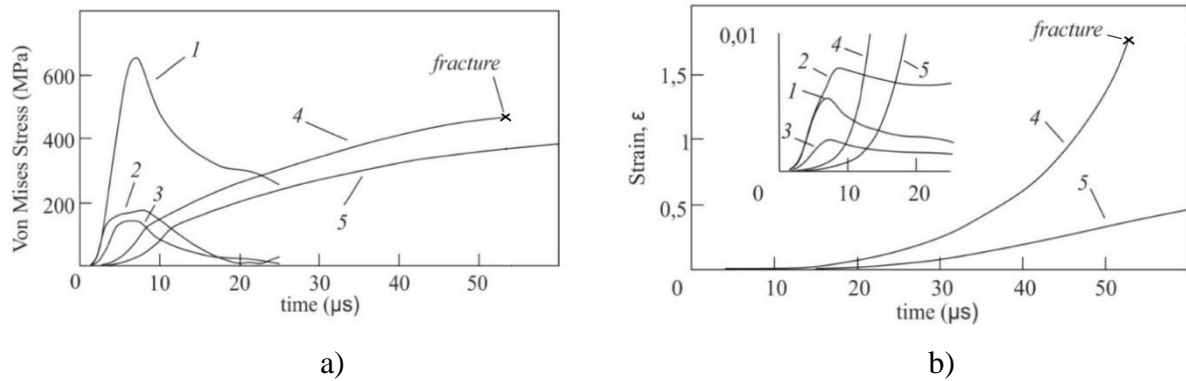


Fig. 4. Von Mises Stress (a) and strain (b) at the groove top.

1 – $P_m = 250$ MPa, $T = 8$ μs (excluding plastic deformation); 2 – $P_m = 250$ MPa, $T = 8$ μs , $\dot{\varepsilon}_p = 1600$ 1/s; 3 – $P_m = 85$ MPa, $T = 8$ μs , $\dot{\varepsilon}_p = 500$ 1/s; 4 – $P_m = 250$ MPa, $T = 50$ μs , $\dot{\varepsilon}_p = 90000$ 1/s; 5 – $P_m = 85$ MPa, $T = 50$ μs , $\dot{\varepsilon}_p = 14000$ 1/s

The results of numerical simulation show that the impact of uniformly distributed pulse pressure on groove, created by MPD, allow to expand strain rate up to 10^5 1/s.

4. Experiment

The experimental setup - the pulse current generator GIT-50/12 was used for experimental study of deformation process [9] with the simple MPD loading scheme (Fig. 1). Current form, measured by Rogowski coil, was damped sinusoid, which can be described by

$$i(t) = I_m \sin\left(\frac{2\pi t}{T}\right) \cdot e\left(\frac{-t}{\tau}\right), \quad (7)$$

where $T = 5.9$ μs , $\tau = 5.6$ μs , the amplitude was determined by the test setup charging voltage, e.g. $I_m = 352$ kA for №4.

Variation of pressure amplitude was reached by changing relation between current amplitude and MPD width. The dependence graph of relative values of groove opening – 1 and precrack – 2 to their initial height $D_i = h_e / h_i$, where h_e , h_i – height of a groove (a

precrack) after the experiment and initial respectively, and pressure amplitude, applied to the groove, relative to the yield stress is shown in Fig. 5.

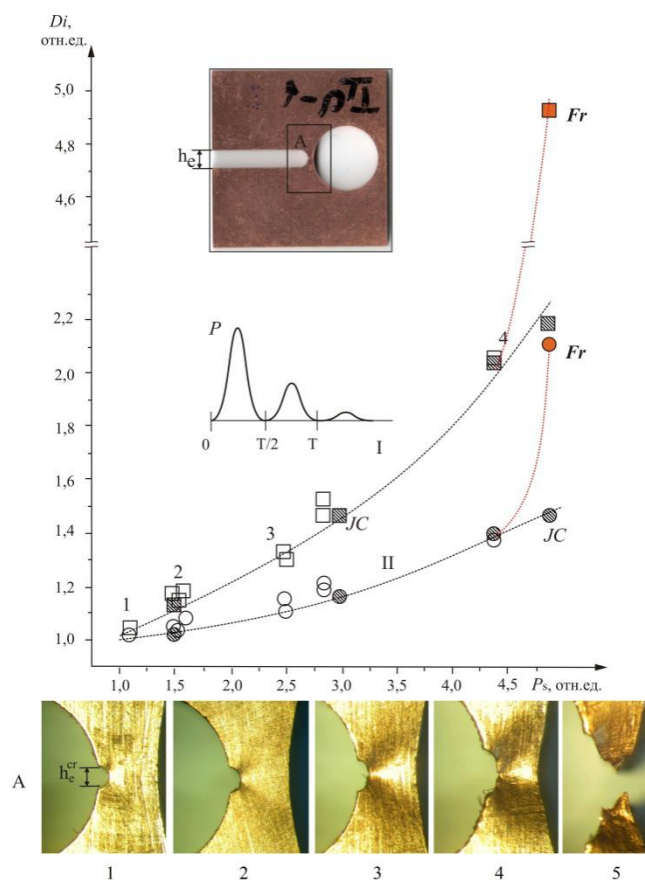


Fig. 5. Dependence graph of relative values of precrack-I groove opening-II and applied pressure relative to the yield stress – $\sigma_y = 90$ MPa; P - pulse pressure form; A – photo of precrack opening of experimental samples; JC – calculated points

Correlation between experimental and simulation results of plastic deformation is shown in figure 5, wherein average average calculated strain rate for the sample №2 was $\sim 3\,300$ 1/s and for the sample №4 was $\sim 10\,000$ 1/s.

Complete fracture after the experiment of the sample №5 is observed (orange points in Fig. 5), whereas the results of calculation with the use of Johnson-Cook criterion for OFHC copper do not correspond conditions of fracture.

Induced current density in the top of the groove of the sample №4 reached ~ 35 kA/mm², oscillation period ~ 5.7 μ s, ratio of near amplitudes ~ 1.29 . Joule heating caused the raise of temperature in the zone with induced current less than 18°C, which according to Johnson-Cook deformation model leads to the reduce of yield stress less than ~ 2 %.

Maximum of magnetic field induction in the top of sample groove reached 4.2 T, which corresponds the amplitude of magnetic pressure equal ~ 9 MPa, while the amplitude of magnetic pressure applied to the shores of the groove reached 421 MPa.

Analysis of experimental results revealed that thermal and force impact of induced currents was insufficient. Since the simulation does not include the impact of electroplastic effect and in the range of relatively low strain rates, experimental data and simulation results have a good correlation; it can be assumed that the impact of electroplastic effect during the action of currents with microsecond duration is not observed within the framework of used method.

It should be noted that in contrast with the data presented in [10–13] where the electroplastic effect was observed at current density 1 kA/mm^2 and impulse duration $60 \mu\text{s}$ and more, the results of experiments with parameters described in this work revealed no impact of electroplastic effect at current densities $\sim 20\text{--}40 \text{ kA/mm}^2$. This may be due to sufficiently less impulse duration or higher strain rate obtained in the experiment.

Further research implies the use of quasi-coaxial MPD, which will allow to exclude the impact of induced currents in the deformation zone, and external current source with the wide range of impulse parameters.

4. Conclusion

Analysis of simulation results showed the possibility of using magnetic-pulse method of deformation of conductive materials at strain rates up to $\sim 100\,000 \text{ 1/s}$.

The results of experimental study have a good correlation with Johnson-Cook model up to strain rate $10^3\text{--}10^4 \text{ 1/s}$, however deviation of calculated parameters from experimental data at the increase of a strain rate can be observed.

Experimental transition to higher strain rates will allow to receive data for Johnson-Cook model verification in a wider range of influences.

Acknowledgments. *The simulation with the use of Comsol Multiphysics and ANSYS autodyn software was carried out at the supercomputer centre "Polytechnic" with heterogeneous cluster HPC Tornado. The parameters of one node of the cluster: RSC Tornado — 2CPU with 14 cores (2× Xeon E5-2697v3 2.6 GHz 64 GB RAM).*

This work is supported by the Russian Science Foundation under grant № 8-19-00230.

Work is supported by the Swiss National Science Foundation (Projects No. 200021_147058 and IZLRZ2-163907/1) and from the Russian Ministry of Education and Science (Project No. RFMEFI58416X0019).

References

- [1] S.I. Krivosheev // *Technical Physics* **50(3)** (2005) 334.
- [2] S.I. Krivosheev, N.F. Morozov, Y.V. Petrov, G.A. Shneerson // *Materials Science* **32(3)** (1996) 286.
- [3] S.I. Krivosheev, G.A. Shneerson, In: *International Conference on Megagauss Magnetic Field Generation and Related Topics, including the International Workshop on High Energy Liners and High Energy Density Applications* (MEGAGAUSS 2008), p. 407. doi: 10.1109/MEGAGUSS.2006.4530709
- [4] S.I. Krivosheev, N.V. Korovkin, V.K. Slastenko, S.G. Magazinov // *International Journal of Mechanics* **9** (2015) 293.
- [5] ANSYS Academic Research Customer, SPbSPU, Perpetual License Number 668315, <http://scc.spbstu.ru/>
- [6] G.R. Johnson, W.H. Cook // *J Eng. Frac. Mech.* **21(1)** (1985) 31.
- [7] V.I. Vas. Balandin, V.I. Balandin, A.M. Bragov, L.A. Igumnov, A.Yu. Konstantinov, A.K. Lomunov // *Mechanics of Solids* **49(6)** (2014) 666.
- [8] S.I. Krivosheev, S.G. Magazinov, D.I. Alekseev // *IEEE trans. on plasma science* **46(4)** (2018) 1054.
- [9] S.I. Krivosheev, S.G. Magazinov, D.I. Alekseev // *MATEC Web of Conferences* **145** (2018) 05006.
- [10] O.A. Troitskii // *Zh. Eksp. Teor. Fiz.* **10(1)** (1969) 18. (in Russian)
- [11] H. Conrad // *Material Science and Engineering* **A322** (2002) 100.
- [12] S. Hameed, H.A.G. Rojas, J.I.P. Benavides, A.N. Alberro, A.J.S. Egea // *Materials* **11(886)** (2018). doi: 10.3390/ma11060886

- [13] Y.R. Ma, H.J. Yang, Y.Z. Tian, J.C. Pang, Z.F. Zhang // *Materials Science & Engineering A* **713** (2018) 146.